 doi:10.20944/preprints201911.0131.v1

Article

The monoclonal antibody recognized apoptosis-associated protein in PCV2-infected peripheral blood mononuclear cells

Ling-Chu Hung [1,2,*] [†]

[1] Animal Health Research Institute, Council of Agriculture, Executive Yuan, 25158 New Taipei, Taiwan; lchung@mail.nvri.gov.tw
[2] Livestock Research Institute, Council of Agriculture, Executive Yuan, 71246 Tainan, Taiwan; lingchuh@mail.tlri.gov.tw
* Correspondence: lchung@mail.nvri.gov.tw; Tel.: +88-6226-212-111
† Current address: Animal Health Research Institute, Council of Agriculture, Executive Yuan, 25158 New Taipei, Taiwan

Abstract: Porcine circovirus type 2 (PCV2) is a small non-enveloped DNA virus that causes swine immunosuppression by inducing apoptosis in lymphocytes. The ORF3 protein plays a major role in PCV2-induced apoptosis in porcine kidney cells, but there is little information regarding this protein in PCV2-infected lymphocytes. In this study, hybridoma screening and epitope mapping were determined by using an indirect ELISA. The mAb 7D3 against ORF3 peptide (residues 35–65) of PCV2 were generated in this study. In vivo situation, the mAb 7D3 recognized ORF3 protein existed in PCV2-infected apoptotic porcine PBMCs. It is noteworthy that thimerosal interfered with the binding of mAb 7D3 to epitope and it was diminished by adding cysteine. Additionally, thimerosal interacting with cysteine-containing peptide was demonstrated by the PTI assay. Furthermore, thimerosal specifically interacted with the antigen-binding sites of mAb 7D3. This study suggested that thimerosal blockade the occlusion of the antigen-binding sites of mAb 7D3 to bind ORF3 peptide (residues 35–65) via thimerosal interacting with cysteine residues which should be located within the antigen-binding sites of mAb 7D3. Overall, the mAb 7D3 has been characterized and it will be a valuables tool in future studies of ORF3 function and the wider mechanism of cell apoptosis caused by PCV2 infection. Similarly, these techniques will be useful for applications in detecting thimerosal too.

Keywords: epitope; monoclonal antibodies; open reading frame 3 protein; apoptosis; p53; porcine circovirus type 2; thimerosal; interfere; antibody binding; lymphocyte

1. Introduction

Porcine circovirus (PCV) is the smallest non-enveloped icosahedral virus and containing a covalently closed circular single-stranded DNA [1]. Previous studies indicated that porcine circovirus type 1 (PCV1) infected-pigs neither showed any signs of illness nor were pathological changes noticeable [2,3]. However, porcine circovirus type 2 (PCV2) infected-pigs showed dull, thin, jaundice, and hepatomegaly, and lesions of the post-weaning multisystemic wasting syndrome (PMWS) [4,5]. Gross lesions associated with PMWS were quite unspecific, but histopathological lesions in lymphoid tissues (lymphocyte depletion with histiocytic infiltration and high concentrations of PCV2) were almost unique for this disease [6]. Likewise, PCV2-associated disease (PCVAD) manifested as severe swine herd problems, including PMWS, porcine dermatitis, and nephropathy syndrome (PDNS), lymphadenopathy, enteritis, and respiratory disease, and reproductive disease [4,7–9].

 doi:10.20944/preprints201911.0131.v1

Open reading frames 1 (ORF1), open reading frames 2 (ORF2), and open reading frames 3 (ORF3) genes are the three major ORFs among 11 ORFs in PCVs[10]. The ORF1 encodes for the replicase proteins Rep and Rep' [10,11]. The major structural capsid protein (CP) is encoded by ORF2 and has a molecular mass of 27.8–30 kDa [10,12]. However, PCV2 is very different from PCV1, especially for the protein encoded by ORF3, which in PCV2 is about half the size of its counterpart in PCV1[10,13]. The ORF3 protein plays a major role in PCV2-induced apoptosis in porcine kidney cells (PK15) by activating initiator caspase-8 and effector caspase-3 pathways [13]. Further, the wild-type PCV2 caused pathological lesions characterized by lymphocyte depletion with histiocytic infiltration of lymphoid organs, but the ORF3-deficient mutant PCV2 failed to induce any obvious pathological lesions in animal experiments [14,15]. In addition, another study demonstrated that the PCV2 ORF3 protein specifically interacted with the porcine p53-induced RING-H2 (pPirh2, an E3 ubiquitin ligase) and inhibited its stabilization in the modulation of cellular function [16]. The data also showed that ORF3 protein competed with p53 in binding to pPirh2, particularly the amino acid residues 20 to 65 of the ORF3 protein were essential in this competitive interaction of ORF3 protein with pPirh2 over p53 [17]. These events contribute to the deregulation of p53 by pPirh2, leading to increased p53 levels and apoptosis of the infected cells [16,17]. Some researcher indicated that ORF3 protein physically interacts with host regulator of G protein signaling 16 (RGS16), leading to degradation of the RGS16 protein, then degradation of RGS16 further enhances NFκB translocation into the nucleus through the ERK1/2 signaling pathway and increases mRNA transcripts of the proinflammatory cytokines IL-6 and IL-8 [18]. Furthermore, the ORF3 protein-induced apoptosis aids in recruiting macrophages to phagocytize the infected apoptotic cells leading to the systemic dissemination of the infection [19]. As a result, the ORF3 protein is possibly the contributing factor for the pathogenesis and lesions associated with PMWS. All known the ORF3 protein characterized to date associate with apoptosis in ORF3-transfected cells and PCV2-infected PK15 cells, raising the question of whether this protein exists in infected apoptotic lymphocytes.

Recently, some researchers try to figure out immunorelevant epitopes of ORF3 protein. The ORF3 peptides (residues 31–50) were proved to be the immunodominant T lymphocyte epitope [20]. Further studies found the linear epitope within the residues 85–95 of the ORF3 protein that was finely defined with synthetic peptides and monoclonal antibodies (mAbs), and they suggested this epitope might be masked in PCV2 infected cells [21,22]. The immunoreactivity of the peptide N1 (residues 35–66) was confirmed by peptides reacting with PCV2-infected pig sera and peptide-immunized mouse sera [23]. Based on previous studies [20,23], there should be epitopes on the N-terminal sequence of ORF3 protein between residues 35 and 66. It would be facile to generate antibodies by utilizing the peptide N1 (residues 35–66) of ORF3 protein. To demonstrate the peptide N1 can mimic the epitopes present on the native ORF3 protein of PCV2b, this study utilized the conjugated N1-KLH to inoculate mice and generate mAbs. This study had generated two mAbs and defined their minimal binding region on peptide N1 using epitope mapping. This study also used immunofluorescence assay to label ORF3 protein and p53 protein to figure out apoptosis in PCV2-infected peripheral blood mononuclear cells (PBMCs).

Thimerosal (merthiolate; sodium ethylmercurithiosalicylate) is an organomercury compound and widely used antiseptic and antifungal agent in some bioproducts, such as vaccines, recombinant proteins, antibodies, ophthalmic products, and so on [24–28]. It is usually advisable to add a preservative, such as 0.01% thimerosal or 0.02–0.05 % sodium azide before sera or antibodies are stored at 4℃ for more than a couple of days. However, sodium azide is a widely used peroxidase inhibitor and could inhibit the horseradish peroxidase (HRP) activity [29]. Consequently, sodium azide-containing is not suitable for HRP conjugation. In this study, some anti-ORF3 protein sera or antibodies were stored at -20℃ with 0.01% thimerosal since no previous research has been reported pertaining to thimerosal affect the antibody binding capacity. While the anti-peptide N1 mAb7D3 had been tested for stability in this storage condition, this study discoverd that thimerosal interferesd with the binding of the mAb 7D3. Hence, this work further elucidates the molecular nature of the interaction of the mAb7D3 and its epitope with thimerosal. Then this study utilized amino acids and

element truncated peptides of N1 to react with thimerosal to identify which essential amino acids of mAb 7D3 or its epitope interact with thimerosal.

2. Results

2.1. Rabbit antisera against the PCV2 peptides

Most rabbits exhibited low background anti-VLP of PCV2 IgG by iELISA before immunization. The antibody titer of each serum (before immunization) were detected at the dilution 1: 100. After five immunizations, the antibody titer was measured in each rabbit serum by iELISA. The peptide N1 and VLP of PCV2 were capable of inducing each specific antibody. The antibody titer of each serum (two weeks after the fourth booster) was detected at the dilution 1: 10,000 (OD value > 0.6 or 0.9). Following iELISA, the IFA test was performed to make sure those antisera could recognize authentic viral protein.

2.2. Hybridomas screening and mAbs production

Mice were immunized with the synthetic peptide (N1). Mice were subsequently euthanized and spleen cells were fused with myeloma cells. Following fusions, hybridoma supernatants were removed and screened for the presence of peptide N1 specific antibodies by iELISA. Among them, 34 hybridoma supernatants reacted with peptide N1 at first screening. After repeatedly subcloning by limiting dilution and screening, two stable hybridomas secreting anti-N1 mAbs (7D3 and 6D10) were obtained.

2.3. Isotyping of anti-N1 mAbs

The isotypes of two mAbs were determined using an SBA ClonotypingTM System/HRP according to the manufacturer's instructions. The hybridoma produced IgG1 mAb (7D3) with kappa-light chains. The other produced mAb (6D10) with lambda-light chains, however, no heavy chain was detected in the supernatant of clone 6D10.

2.4. Mapping of anti-N1 mAb epitopes

Peptides included the N-terminal sequence of PCV2 ORF3 protein between residues 35 and 66, associated 10-mer peptides, and truncated derivatives. Two mAbs bound to the N-terminal sequence of PCV2b ORF3 protein (peptide N1, C_{35}HNDVYISLPITLLHFPAHFQKFSQPAEISDKR$_{66}$). To determine the binding site of each mAb, a peptide scan analysis was performed (Figure 1). The mAb 7D3 just bound to the linear epitope (P126, $_{35}$HNDVYISLPITLLHFPAHFQKFSQPAEISDKR$_{66}$) without an N-terminal cysteine compared to the peptide N1. However, the non-IgG mAb (6D10) showed moderate reactions against all peptides in the ELISA test (Figure 1).

Preprints (www.preprints.org) | NOT PEER-REVIEWED | Posted: 12 November 2019 doi:10.20944/preprints201911.0131.v1

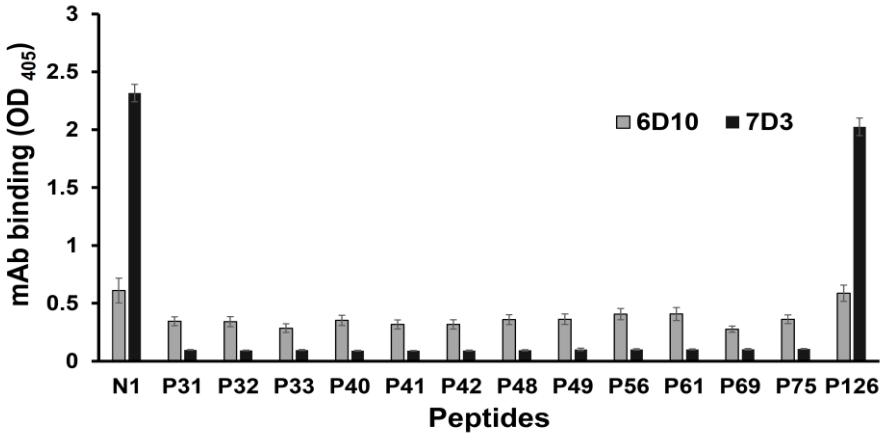

Figure 1. Determination of linear epitope binding for anti-N1 mAbs. Anti-N1 mAbs (7D3 and 6D10) bound the linear peptide spanning from residues 35 to 66 and tested for mAbs binding using an iELISA. Peptides contained the N-terminal sequence of PCV2 ORF3 protein between residues 35 and 66, associated 10-mer peptides (spanning the peptide N1 and overlapping by five residues at a time), and truncated derivatives (as shown in Table 1). Data represent the mean ± SEM and are representative of three independent assays.

2.5. Nuclear morphological changes in some PCV2-infected PBMCs

For the homemade PBMCs slides, all wells contained both negative and positive cells (PCV2-infected cells) were confirmed by IFA, as previously noted in a similar study [30]. As previous work demonstrated that anti-C3 mAbs (1H3, 3B2, and 6B8) recognized native capsid protein and reacted with core peptide (P59, $_{227}$KDPPLNP$_{233}$), but these mAbs produced variable positive staining pattern in PBMCs by IFA [30]. In this study, PCV2 viral proteins (ORF3 protein and capsid protein) location were initially assessed by IFA. These home-made polyclonal rabbit antibodies and mAb (7D3) were colocalized with anti-C3 mAbs (1H3, 3B2, and 6B8) and conventional anti-capsid mAb (36A9). Interesting, the anti-VLP of PCV2 rabbit serum produced cytoplasmic staining with rare intranuclear staining in PCV2-infected PBMCs (Figure 2B, F, J). When PCV2-infected PBMCs were co-stained with anti-VLP of PCV2 rabbit serum and anti-C3 mAbs (3B2 and 6B8), some VLP/C3 dual-positive cells were showed abnormally or small shape nuclei (Figure 2C, G). Similarly, PCV2-infected PBMCs were co-stained with anti-VLP of PCV2 rabbit serum and anti-N1 mAb 7D3, some VLP/N1 dual- positive cells were also showed abnormally or small shape nuclei (Figure 2K).

The previous study suggested that ORF3 protein is leading to increased p53 levels and apoptosis of the infected cells [31]. To identify the subcellular location of ORF3 protein in PCV2-infected PBMCs, among anti-C3, anti-N1, and anti-p53 antibodies were used. This result showed peptide N1 close to the capsid protein marker of PCV2 (Figure 2L, 3H). p53 also colocalized with peptide C3 (Figure 3D) and N1 (Figure 4D). It is noteworthy that p53 protein was mainly distributed in the cytoplasm and some distributed as a flocculent in the nucleus (Figure 3D, 4D). The p53/N1 dual-positive cell was showed abnormally and segmented nucleus (Figure 4A, E). Nuclei of negative cells were round or oval, and nuclear segmentation was very rare in negative cells (Figure 4F). Taken together, these findings indicate that the frequency of irregular nuclear shape is more severe in strong dual-positive cells compared with weak positive or negative cells (Figure 2H, 2L, 3D, and 4F).

 doi:10.20944/preprints201911.0131.v1

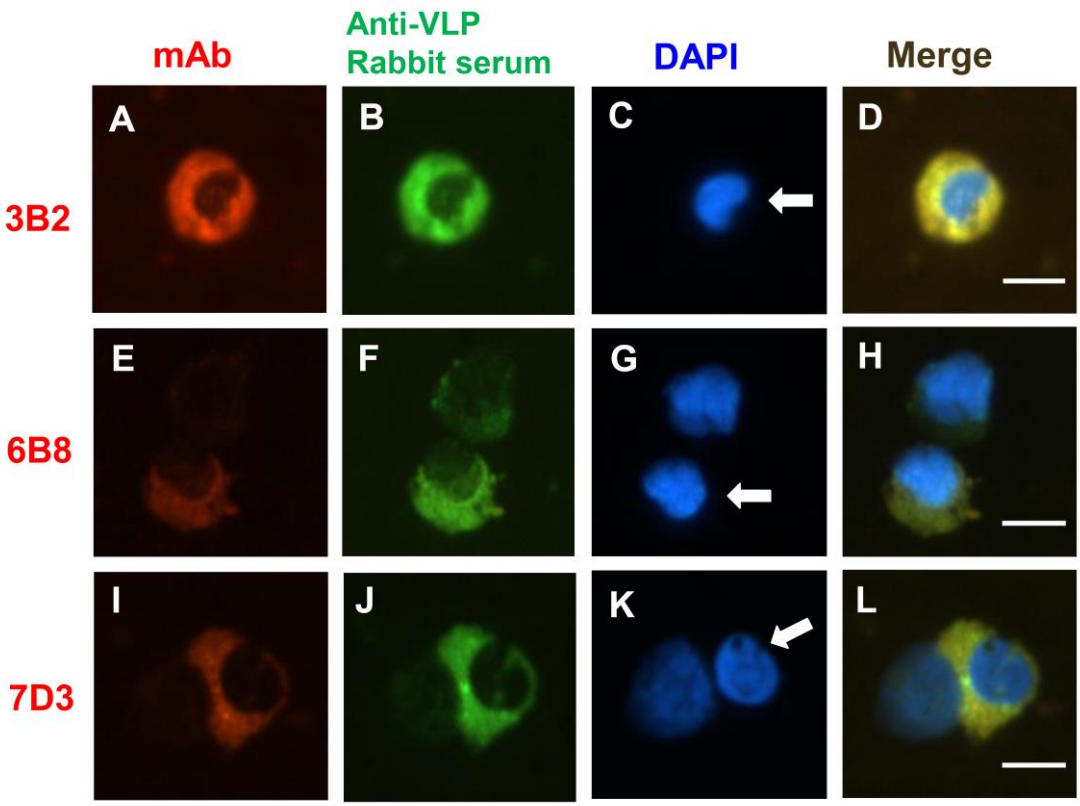

Figure 2. Localization of viral proteins of PCV2 on PCV2-infected PBMC. Localization of viral proteins of PCV2 was assessed by indirect IFA using anti-VLP of PCV2 rabbit serum (green) and costaining with mouse mAbs (red) to mark various viral epitopes: anti-C3 mAb 3B2 (KDPPLNP), anti-C3 mAb 6B8 (KDPPLNP and KDPPLNP**K**), or anti-N1 mAb 7D3 (HNDVYISLPITLLHFPAHFQ KFSQPAEISDKR). Left column (A, E, and I): Staining with mouse mAbs (red) was used to identify the capsid protein of PCV2 (A and E) and the ORF3 protein of PCV2 (I). The second column from the left (B, F, and J): Fluorescence microscopy of VLP of PCV2 were identified (green). The third column from the left (C, G, and K): Nuclei were stained with DAPI (blue), some dual-positive cells were showed abnormally or small shape nuclei (arrows). Right column (D, H, and L): The merge of the images is shown. Scale bars, 10 μm.

Preprints (www.preprints.org) | NOT PEER-REVIEWED | Posted: 12 November 2019 doi:10.20944/preprints201911.0131.v1

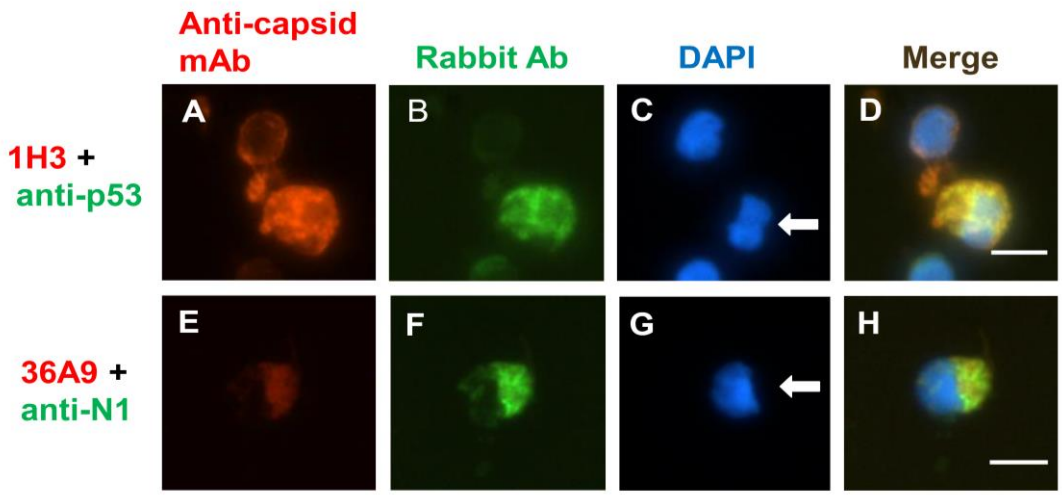

Figure 3. Subcellular location of the ORF3 protein and p53 in PCV2-infected PBMCs. Localization of capsid proteins of PCV2 was assessed by indirect IFA using mouse mAbs (red) to mark capsid epitopes: anti-C3 mAb 1H3 (DPPLNP, DPPLNP**K**, LKDPPL**K**P), or anti-capsid mAb 36A9. Left column (A and E): Staining with mouse mAbs (red) was used to identify the capsid protein of PCV2. The second column from the left (B and F): Costaining with rabbit antibody (green) was used to identify p53 (B) or the ORF3 protein of PCV2 (F). Nuclei were stained with DAPI (blue, C and G), some dual-positive cells were presented abnormally or small shape nuclei (arrows). The merge of the images is shown (D and H). Scale bars, 10 μm.

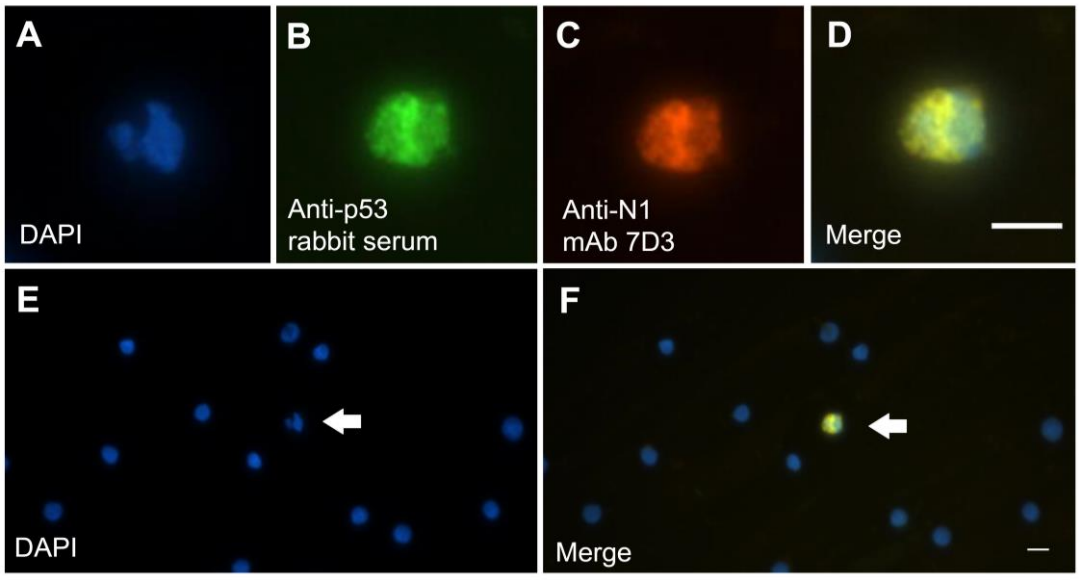

Figure 4. Morphological abnormality in PCV2-infected PBMCs. Immunofluorescence microscopy of PCV2-infected PBMCs with antibodies against p53 (green) and N1 (red). Left column (A and E): Nuclei were stained with DAPI, the arrow pointed to the irregularly shaped nucleus (E), and enlarged in the upper left panel (A). Staining with rabbit antibody (green) was used to identify p53 (B). Costaining with mAb 7D3 (red) was used to identify the ORF3 protein of PCV2 (C). The merge of the images is shown (D and F). Scale bars, 10 μm.

Preprints (www.preprints.org) | NOT PEER-REVIEWED | Posted: 12 November 2019 doi:10.20944/preprints201911.0131.v1

2.6. Thimerosal interfere with mAb 7D3 binding to peptide N1

To determine whether preservative could interfere with the specific mAb binding to the linear epitope, two common preservatives (thimerosal and sodium azide) and four mAbs (7D3, 3B2, 8A3, and 6D10) were used in this study. The mAb 7D3 specific bound the peptide N1, whereas the mAb 7D3 mixed with 0.1% thimerosal content (1000 μg/mL, just as 100 μg/well) that decreased significantly the strength of the interactive binding of mAb 7D3 and peptide N1 compared with the non-treated control did ($p < 0.05$; Figure 5A). Otherwise, 0.1% thimerosal content did not interfere with other mAbs (3B2, 8A3, and 6D10) binding to their linear epitopes in this test (Figure 5A, B). Similarly, 0.1% sodium azide content did not interfere with mAbs (3B2, 8A3, 7D3, and 6D10) binding to their linear epitopes in this test (Figure 5A, B). Further, to estimate the concentration of thimerosal interfere with antibodies (mAbs or mouse antisera) binding to the linear epitope, thimerosal at various concentrations was mixed with antibodies (ascites or sera were used at 1:1000 dilution). The data indicated that mAb 7D3 with high thimerosal (≧10 μg/well, just as ≧100 μg/mL) content decreased significantly the strength of the interactive binding of peptide N1 and mAb 7D3 compared with mAb 7D3 with low thimerosal (≦1 μg/well, just as ≦10 μg/mL) content did ($p < 0.05$; Figure 6A). However, anti-N1 mouse serum with high thimerosal content did not change significantly the strength of the interactive binding of peptide N1 and anti-N1 polyclonal antibody compared with anti-N1 mouse serum without thimerosal content did ($p > 0.05$; Figure 6A). Similarly, anti-C3 antibodies (mAb 8A3 or anti-C3 mouse serum) with thimerosal content did not change significantly the strength of the interactive binding of peptide C3 and anti-C3 antibodies compared with anti-C3 antibodies (mAb 8A3 or anti-C3 mouse serum) without thimerosal content did, except antibodies (mAb 8A3 or anti-C3 mouse serum) with thimerosal level at 10 μg/mL (1 μg/well) did (Figure 6B).

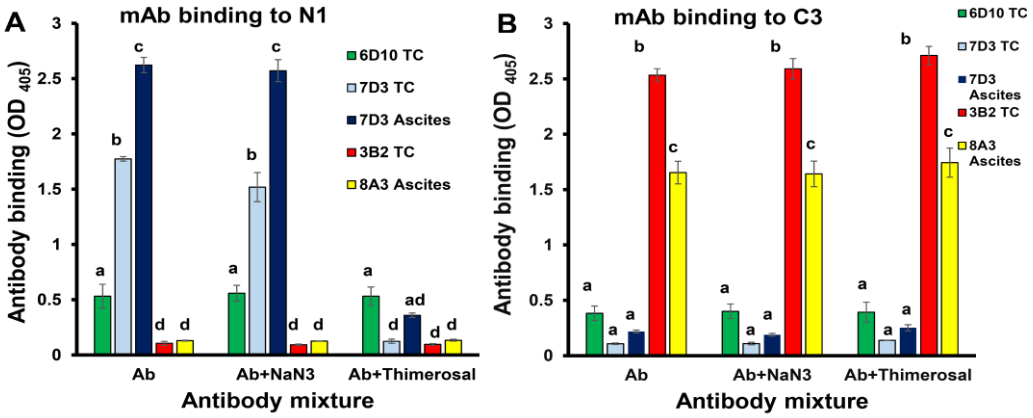

Figure 5. Assessment of preservative affecting specific mAb-peptide binding by IIDM. Evaluation of preservative (thimerosal or sodium azide) affects binding potencies of anti-N1 mAbs (6D10 and 7D3) and anti-C3 mAbs (3B2 and 8A3). ELISA plates were coated with the peptide N1 (A), and the others were coated with the peptide C3 (B). Each mAb with 0.1% preservative content was then tested for reactivity against the N1 coated plate (A) and C3 coated plate (B), respectively. Statistic calculations were done using one-way ANOVA with Tukey's Studentized Range (HSD) multiple comparisons test. A p-value < 0.05 was considered significant. Data represent the mean ± SEM and are representative of three independent assays. Treatments with different letters have statistically significant differences.

Preprints (www.preprints.org) | NOT PEER-REVIEWED | Posted: 12 November 2019 doi:10.20944/preprints201911.0131.v1

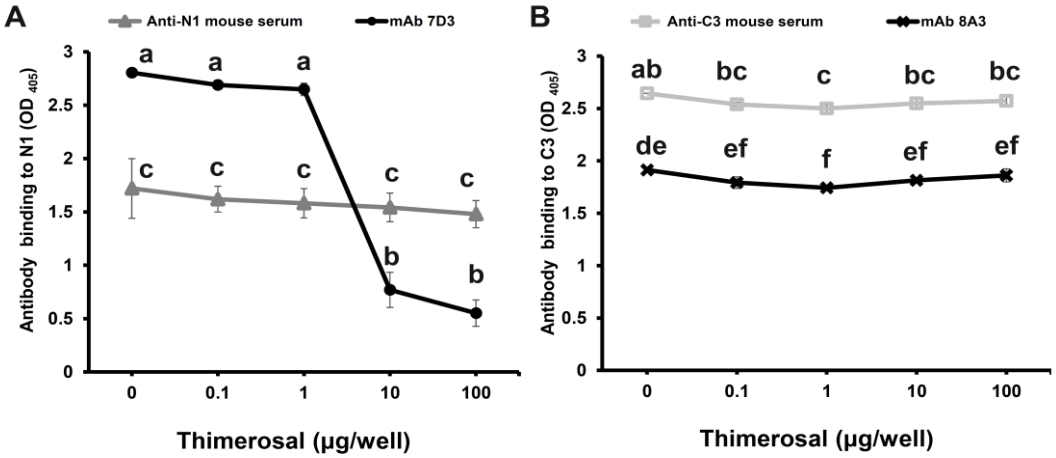

Figure 6. Effect of thimerosal on the binding of specific antibodies to linear peptides. ELISA plates were coated with the peptide N1 (A), and the others were coated with the peptide C3 (B). Antibodies with different concentrations of the thimerosal were tested for reactivity against the N1 coated plate (A) and C3 coated plate (B), respectively. Statistic calculations were done using one-way ANOVA with Tukey's Studentized Range (HSD) multiple comparisons test. A p-value < 0.05 was considered significant. Data represent the mean ± SEM and are representative of three independent assays. Treatments with different letters have statistically significant differences.

2.7. Cysteine inhibits the interaction of thimerosal with mAb 7D3

To better understand how thimerosal influences the strength of the interactive binding of mAb 7D3 and its linear epitope, the assay of thimerosal interacting-truncated peptides of N1 and amino acids were performed using bIIDM. This assay is based upon specific blocking of thimerosal by preincubating with truncated peptides of peptide N1 or amino acids. Although all of the truncated peptides (at 5 µg/well) tested for inhibiting active site of thimerosal were used in a concentration 10-fold higher than that of coating peptide N1 (at 0.5 µg/well), they did not diminish the strength of thimerosal (at 100 µg/well) interfering with the binding of mAb 7D3 to peptide N1 (Figure 7).

To further evaluate which critical residues within the mAb 7D3 (or its linear epitope) were particularly important for interaction with thimerosal. In the following experiments, the peptide P126 was used at 0.5 µg/well to coat ELISA plates. Thirteen of the amino acids were tested for their ability to interact with thimerosal in this assay. Among them, only cysteine (at 500 µg/well) diminished the strength of thimerosal (at 100 µg/well) interfering with the binding of mAb 7D3 to the peptide P126 (p < 0.05, compared to the result for the control group) (Figure 8). Since the peptide P126 ($_{35}$HNDVYISLPITLLHFPAHFQKFSQPAEISDKR$_{66}$) does not contain cysteine residue, one attractive possibility is that cysteine interacted directly with thimerosal to quench thimerosal interfering with the binding of mAb 7D3 to the peptide P126.

Preprints (www.preprints.org) | NOT PEER-REVIEWED | Posted: 12 November 2019 doi:10.20944/preprints201911.0131.v1

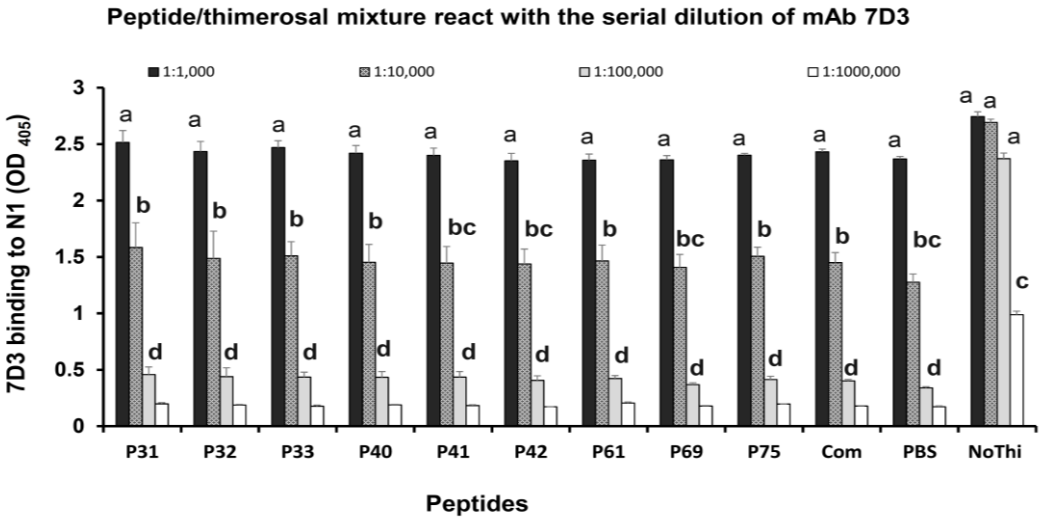

Figure 7. Assessment of thimerosal interacting-truncated peptides of N1. The determination of thimerosal interacting-element peptide of N1 was assessed by bIIDM using a serial dilution of mAb 7D3. All of the truncated peptides (at 5 μg/well) tested for inhibiting active site of thimerosal were used in a concentration 10-fold higher than that of coating peptide N1 (at 0.5 μg/well). Com (combined P31, P32, P33, P40, P41, and P42) was included in this experiment. PBS (no peptide) was used as a negative control. No Thi (neither thimerosal nor peptide) was used as a positive control. Statistic calculations were done using one-way ANOVA with Tukey's Studentized Range (HSD) multiple comparisons test. A p-value < 0.05 was considered significant. Data represent the mean ± SEM and are representative of three independent assays. Treatments with different letters have statistically significant differences.

Preprints (www.preprints.org) | NOT PEER-REVIEWED | Posted: 12 November 2019 doi:10.20944/preprints201911.0131.v1

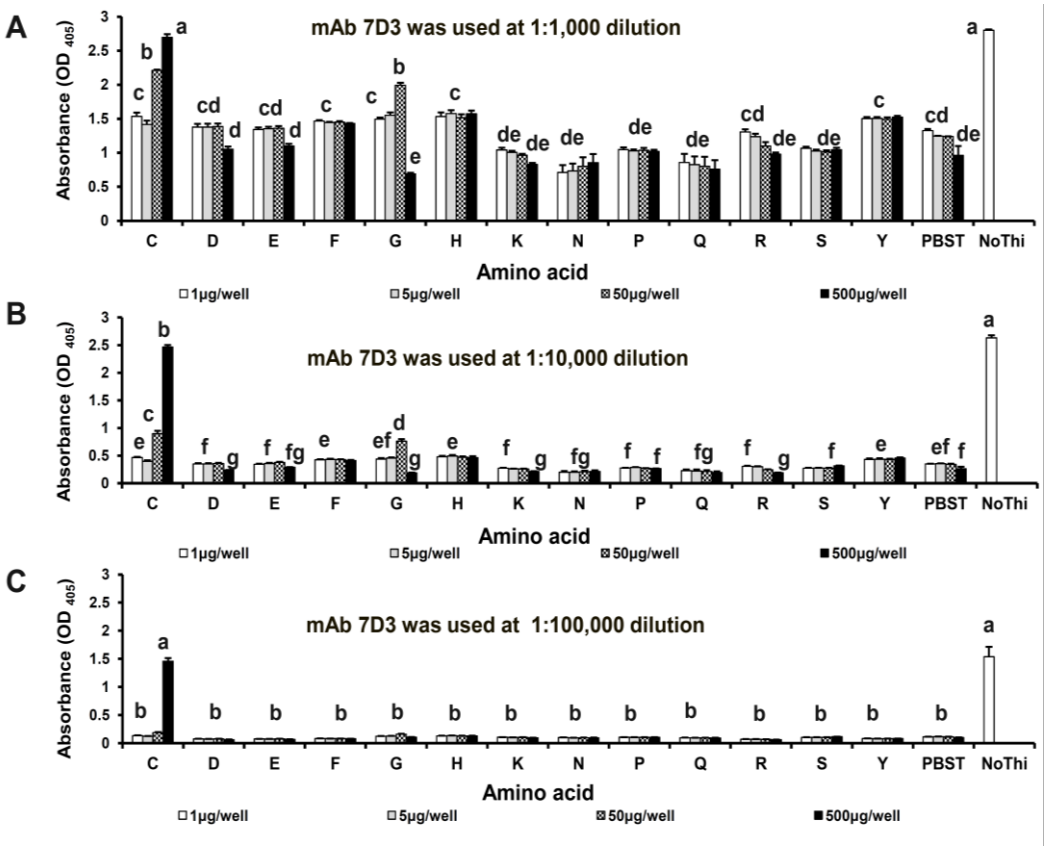

Figure 8. Determination of thimerosal interacting-amino acids. The peptide P126 was used at 0.5 µg/well to coat ELISA plates. Arginine (R), asparagine (N), aspartic acid (D), cysteine (C), glutamine (Q), glutamic acid (E), glycine (G), histidine (H), lysine (K), phenylalanine(F), proline (P), serine (S), and tyrosine (Y) were tested for their ability to interact with 0.1 % thimerosal. Determination of thimerosal interacting-amino acid was assessed by bIIDM using a serial dilution of mAb 7D3 and amino acids within the range of concentration (up to 5 mg/mL, 100 µL per well). PBST (no amino acid) was used as a negative control. No Thi (neither thimerosal nor amino acid) was used as a positive control. Statistic calculations were done using one-way ANOVA with Tukey's Studentized Range (HSD) multiple comparisons test. A p-value < 0.05 was considered significant. Results show the mean of three assays, each with two replicate wells. Error bars indicate standard deviations. Treatments with different letters have statistically significant differences.

2.8. Thimerosal interacts with cysteine-containing peptide

Having shown that cysteine achieved a reduction in the interaction of thimerosal with mAb 7D3, this study hypothesized that this activity may be related to the ability of cysteine to block the interaction of thimerosal with cysteine-containing peptide or mAb 7D3. The following experiment was set up to investigate whether cysteine-containing peptide was capable of interacting with thimerosal. The interaction was detected by coating peptide using cysteine-containing peptide (peptide N1) in the PTI assay, but not by coating peptide using a cysteine-free epitope (peptide P126) in the PTI assay (Figure 9). The result indicated that coating peptide using thimerosal-treated peptide N1 (cysteine-containing peptide) diminished the strength of mAb 7D3 binding to the peptide N1 (p < 0.05, compared to the result for the control group) (Figure 9). However, coating peptide using thimerosal-treated P126 (cysteine-free epitope) did not diminish the strength of mAb 7D3 binding to the peptide P126 (p > 0.05, compared to the result for the control group) (Figure 9).

Preprints (www.preprints.org) | NOT PEER-REVIEWED | Posted: 12 November 2019 doi:10.20944/preprints201911.0131.v1

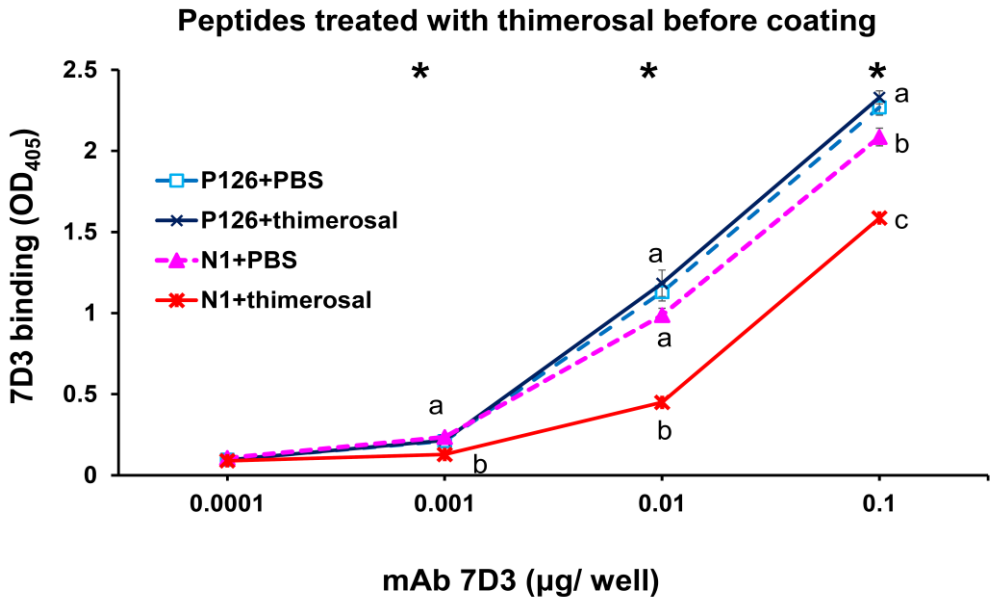

Figure 9. Assessment of cysteine-containing peptide interacting with thimerosal by PTI assay. Thimerosal-treated peptides were used as coating antigens. The mAb 7D3 was used within the range of concentration (up to 0.1 µg/well, 100 µL per well). Statistic calculations were done using one-way ANOVA with Tukey's Studentized Range (HSD) multiple comparisons test. Results show the mean of two independent experiments (hexplicate wells). Error bars indicate standard deviations. Significant *p* values are indicated as * $p < 0.05$. Treatments with different letters have statistically significant differences at that concentration.

2.9. Thimerosal diminishes the strength of mAb 7D3 binding

Having demonstrated that thimerosal interacted with cysteine-containing peptide (N1) in the PTI assay, but not cysteine-free epitope (P126). Although thimerosal does not interact with P126, previous data showed that thimerosal interferes with mAb 7D3 binding to the peptide P126. Therefore this study suggested that thimerosal may directly interact with mAb 7D3 and diminish the strength of its binding to the peptide P126. The following experiment was set up to clarify the relationship between the concentration of thimerosal and the strength of mAb 7D3 binding to the peptide P126. In order to estimate the concentration of thimerosal diminishes the strength of mAb 7D3 binding to its cysteine-free epitope, thimerosal at various concentrations (range from 0 µg/well to 1000 µg/well) was mixed with mAb 7D3 (range from 0.0001 µg/well to 1 µg/well) in this experiment. The data indicated that mAb 7D3 (≦0.1 µg/well, just as ≦1 µg/mL) with thimerosal (≧1 µg/well, just as ≧10 µg/mL) content decreased significantly the strength of the interactive binding of mAb 7D3 and peptide P126 compared with mAb 7D3 without thimerosal content did ($p < 0.05$; Figure 10A). However, mAb 1H3 even with 1 % thimerosal (1000 µg/well, just as 10 mg/mL) content did not change significantly the strength of the interactive binding of mAb 1H3 and peptide P59 compared with mAb 1H3 without thimerosal content did ($p > 0.05$; Figure 10B). Owing to both mAb 1H3 and mAb 7D3 belonged to the IgG1 isotype with kappa (κ) light chains, the antigen-binding sites of immunoglobin were the only difference between these two mAbs.

Preprints (www.preprints.org) | NOT PEER-REVIEWED | Posted: 12 November 2019 doi:10.20944/preprints201911.0131.v1

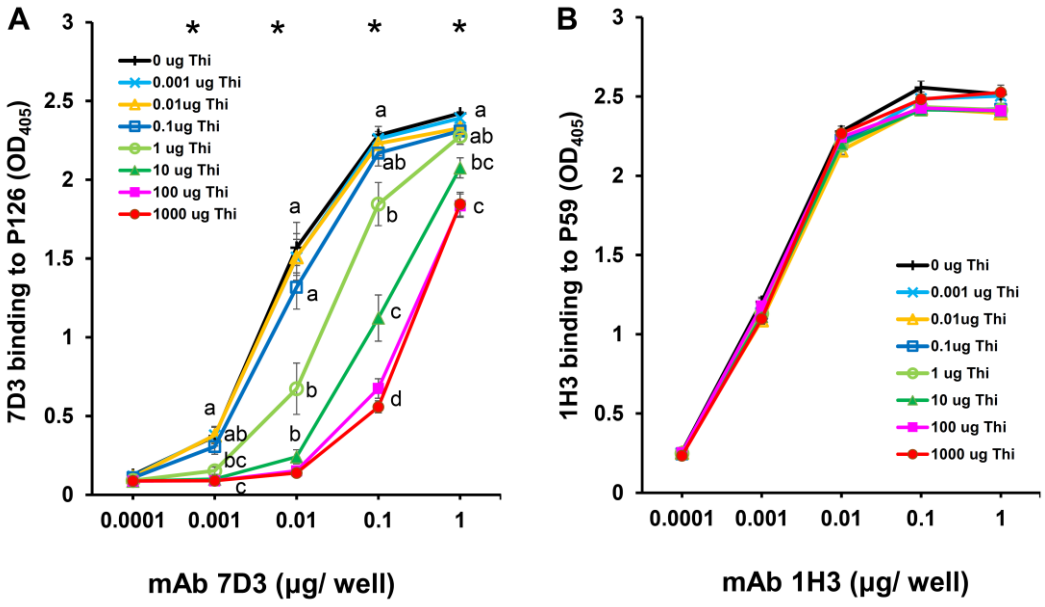

Figure 10. Quantification of mAb and thimerosal interaction by IIDM. To estimate the effect of thimerosal (Thi) on the binding of specific mAb to a linear epitope in the liquid phase. (A) mAb 7D3 was tested for binding to P126 (0.5 µg/well) with thimerosal concentrations ranging between 0 and 1,000 µg/well (100 µL per well). (B) mAb 1H3 was tested for binding to P59 under the same conditions. Statistic calculations were done using one-way ANOVA with Tukey's Studentized Range (HSD) multiple comparisons test. All experiments were repeated three times, and average values are shown. Error bars indicate standard deviations. Significant p values are indicated as * $p < 0.05$. Treatments with different letters have statistically significant differences at that concentration.

 doi:10.20944/preprints201911.0131.v1

3. Discussion

Researchers demonstrated that ORF3 deletion mutants 20–50 and 35–65 neither induced apoptosis in the transfected cells nor interacted with pPirh2, they suggested that the region containing the 20th to 65th amino acid residues causes apoptosis in PCV2-infected cells and could be important in the interaction between pPirh2 and p53 [31]. The 35th to 66th amino acid residues of ORF3 protein (peptide N1) was synthesized and proved to be the immunodominant peptide [23]. In order to search fine epitopes on the peptide N1, this study utilized the conjugated N1-KLH to inoculate mice and generate hybridomas. This work generated one hybridoma producing IgG1 mAb, the other hybridoma producing immunoglobulin without heavy chains. The IgG1 mAb 7D3 bound to the linear peptide N1 (C_{35}HNDVYISLP ITLLHFPAHFQKFSQPAEISDKR$_{66}$) and P126 ($_{35}$HNDVYISLPITLLHFPAHFQK FSQPAEISDKR$_{66}$). However, the defected Ig mAb 6D10 almost reacted with all truncated peptides. This finding is similar to the previous study [30], it's probably that defected Ig mAb have broadly binding with associated peptide.

Previous IFA data for PCV2-infected PBMCs have shown that anti-C3 mAbs (1H3, 3B2, and 6B8) produced positive staining reaction in homemade IFA slides [30], so this study used both polyclonal anti-N1 rabbit serum and anti-N1 mAb 7D3 (binding residues 35–66) to observe ORF3 protein of PCV2 in PCV2-infected PBMCs by colocalization with markers of capsid protein of PCV2 and p53 marker of apoptosis. In this approach, some VLP/C3 dual-positive cells were showed abnormally or small shape nuclei, and some capsid/N1 dual-positive cells were also showed small bizarre nuclei. It is implied that PBMCs could undergo PCV2 infection then reacted by causing pyknosis or apoptosis. According to previous studies, exogenous ORF3 protein interacts with pPirh2 and leads to increasing p53 levels and apoptosis in ORF3-transfected PK15 cells, PCV2-infected PK15 cells, and ORF3-transfected H1299 cells [16,17]. Recent research has shown that PCV2 induced S phase accumulation through p53 mediated up-regulation of p21, Cyclin E and down-regulation of Cyclin A, CDK 2 proteins in PK15 cells [32]. Nevertheless, lymphocyte depletion and apoptosis in lymphoid tissues are histological hallmarks in PCV2-infected pigs [33–36]. Lymphocyte and PBMCs lineage cells should be the major target cells for PCV2 infection. To the best of the author's knowledge, the ORF3 protein study by indirect immunofluorescence assay in PCV2-infected PBMCs had never been performed and only a single article mentioned the transient expression of ORF3 in porcine PBMCs and detecting apoptosis with TUNEL assay [37]. Therefore this work explored the relation of pyknosis and peptide N1 (residues 35–66) of ORF3 protein by IFA, and shed light on residues 35–66 of ORF3 protein was accompanied by p53 protein in PCV2-infected PBMCs. The result indicated residues 35–66 of ORF3 protein close to the capsid protein marker of PCV2. p53 protein colocalized with residues 35–66 of ORF3 protein. The p53/N1 dual-positive cell was presented segmented nucleus which was similar to apoptosis (Figure 4). These IFA data confirm previous reports that exogenous ORF3 protein was related to the accumulation of p53 [16,17] and agree with previous studies showing that ORF3 protein was associated with apoptosis phenomena in PCV2-infected cells or ORF3-transfected cells [17,38,39].

Many scientists routinely add sodium azide or thimerosal as an anti-microbial agent to all preparations of antibodies in order to inhibit microbial growth. Although it is well known that antibodies containing preservatives must be stored at ≤ 4 ℃ in sterile polypropylene tubes, most researchers were not even aware that these preservatives could affect the antibody binding capacity. To address the above-mentioned hypothesis, two common preservatives (thimerosal and sodium azide) and four mAbs (three IgG1 mAbs and one defective Ig mAb) were tested by IIDM assay to clarify whether preservative could interfere with the specific mAb binding to its epitope. The data indicated that only mAb 7D3 with greater than or equal to 0.01% thimerosal (≧10 μg/well) content decreased the strength of the interactive binding of peptide N1 and mAb 7D3. Otherwise, 0.1% thimerosal content did not decrease other mAbs (3B2, 8A3, and 6D10) binding to their linear epitopes in the same test. Similarly, 0.1% sodium azide content did not affect mAbs (3B2, 8A3, 7D3, and 6D10) binding to their linear epitopes in the same assay. Notably, these mAbs (3B2, 8A3, and 7D3) belonged

 doi:10.20944/preprints201911.0131.v1

to the IgG1 isotype with kappa(κ) light chains, but each mAb bound to the different minimal linear epitope [30]. This observation raises the hypothesis that thimerosal may interact with key amino acid residues within the antigen-binding site of mAb 7D3 or peptides (N1 or P126), then it blocks mAb 7D3 binding to peptides (N1 or P126).

According to the previous study [40], thimerosal decomposes into thiosalicylic acid and ethylmercury in aqueous media. An earlier report on mercury-binding proteins of Mytilus edulis described these proteins had similar amino acid compositions with 26% half-cystine, 16% glycine, and very low levels of the aromatic amino acids phenylalanine and tyrosine (0.3–0.5%), histidine (0.4%), methionine (0.5%), and leucine (1%) [41]. To evaluate which critical residues within the mAb 7D3 (or its linear epitope) were particularly important for interaction with thimerosal, the assay of thimerosal interacting-amino acids was performed using bIIDM. This assay was invented by the author of this paper and based upon specific blocking of thimerosal by preincubating with amino acids before thimerosal interacted with mAb 7D3 or peptide P126. According to the compositions of peptide P126 and mercury-binding proteins of Mytilus edulis, arginine, asparagine, aspartic acid, cysteine, glutamine, glutamic acid, glycine, histidine, lysine, phenylalanine, proline, serine, and tyrosine were used in this assay. These results demonstrated only cysteine (at 500 μg/well) diminished the strength of thimerosal (at 100 μg/well) interfering with the binding of mAb 7D3 to the peptide P126. This research suggested that cysteine interact directly with thimerosal to quench thimerosal interfering with the binding of mAb 7D3 to the peptide P126. Additionally, thimerosal interacting with cysteine-containing peptide was demonstrated by coating the peptide N1 (peptide N1 was appended with cysteine at N-terminus of peptide P126 during synthesis) in the PTI assay, but it was not detected by coating the peptide P126 (cysteine-free peptide) in the PTI assay (Figure 9). This agrees with previous studies showing that thimerosal interacts with cysteine-containing proteins via ethylmercury moiety binding to the free thiol group of proteins [42] and it leads to changing protein conformation [43] and altering its antigenicity and immunogenicity [44].

Although thimerosal does not interact with peptide P126 (cysteine-free peptide) in the PTI assay (Figure 9), the aforementioned data showed that thimerosal interferes with mAb 7D3 binding to the peptide P126 in the bIIDM assay (Figure 8). Hence this study postulated that thimerosal may be interacted with cysteine residues within the antigen-binding sites of mAb 7D3 and diminished the strength of its binding to the peptide P126. To bear out this hypothesis, this study used another mAb 1H3 (IgG1 isotype with kappa light chains) for negative control. This study indicated that mAb 7D3 with thimerosal (≧10 μg/mL) content decreased significantly the strength of the interactive binding of mAb 7D3 and peptide P126 compared with mAb 7D3 without thimerosal content did (Figure 10A). Conversely, mAb 1H3 even with 1 % thimerosal (10 mg/mL) content did not change significantly the strength of the interactive binding of mAb 1H3 and peptide P59. These results revealed that thimerosal specifically interacted with mAb 7D3. Since both of mAb 7D3 and mAb 1H3 belong to the same isotype and individual mAbs differ in their variable regions of immunoglobulin, especially in their antigen-binding sites. Previous data also showed that the only cysteine diminished the strength of thimerosal interacting with mAb 7D3. Therefore this study suggested that thimerosal blockade the occlusion of the antigen-binding sites of mAb 7D3 to bind peptide P126 via thimerosal interacting with cysteine residues which were located within the antigen-binding site of mAb 7D3. Further research should be carried out advanced techniques (such as liquid chromatography with mass spectrometry and spectroscopic techniques) to investigate free thiols within the antigen-binding sites of mAb 7D3 and evaluate the interaction between mAb 7D3 and thimerosal simulating physiological conditions.

On the basis of previous studies that showed the regions of Pirh2 encompassing residues 120–137 and 249–256 which were required for binding p53 [16,45,46], then the scientists discovered that the ORF3 protein of PCV2 interacted with the p53-binding domain of pPirh2 (residues 120 to 137) and facilitated p53 expression in PCV2 infection [16]. Subsequently, researchers demonstrated that the ORF3 protein with deletions in the amino acid residues 20–50 and 35–65 did not interact with pPirh2 as efficiently as wild-type ORF3 protein or other ORF3 deletion mutants [17]. They suggested

Preprints (www.preprints.org) | NOT PEER-REVIEWED | Posted: 12 November 2019 doi:10.20944/preprints201911.0131.v1

that the ORF3 efficiently disrupt the p53 homeostasis by interacting with Pirh2, through its amino acid residues 20–50 and 35–65. These p53-binding sites and the ORF3 protein-interacting site of Pirh2 are illustrated in Figure 11. Intriguingly, each site contains cysteine residues. It is implied the thiol group of cysteine that might play a role in the binding affinity [47–49] of Pirh2 (residues 120–137 and 249–256) to ORF3 protein (residues 20–50 and 35–65) as well as mAb 7D3 to the peptide P126 (ORF3 protein residues 35–65). Both of Pirh2 and mAb 7D3 bind to the same peptide of ORF3 protein (residues 35–65). Pirh2 binds to ORF3 protein which caused by PCV2-infection. However, mAb 7D3 was generated by immunological methods and hybridoma screening which was selected specifically binding to the 35th to 66th amino acid residues of ORF3 protein. Therefore, further investigation of the amino acid sequence of the antigen-binding sites of mAb 7D3 would be interesting.

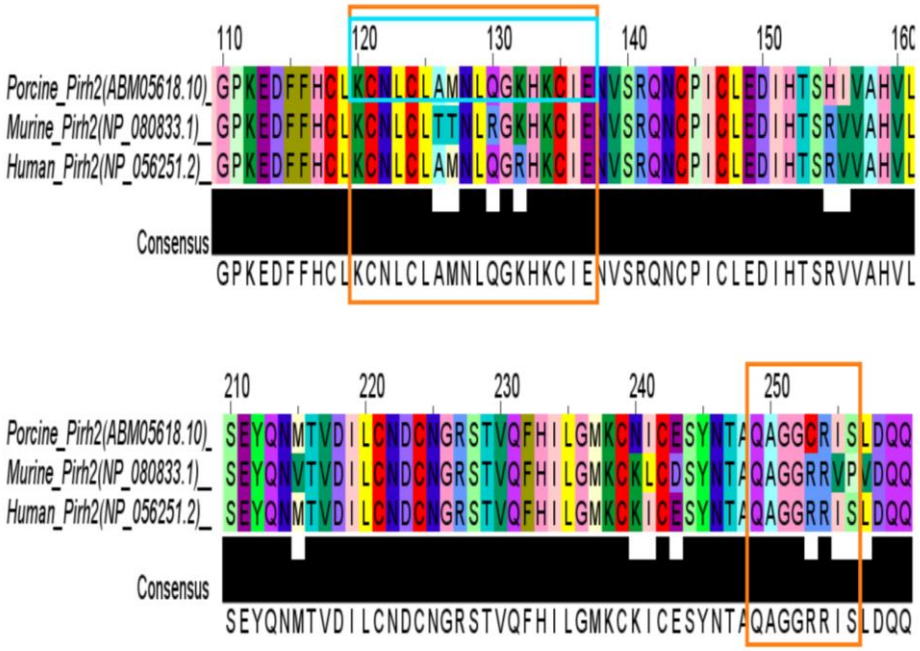

Figure 11. Amino acid Sequence alignments of the Pirh2 from three species of animals were used. The amino acid residues of the p53-binding domain of pPirh2 locate in the orange box. The ORF3 protein-interacting site of porcine Pirh2 is illustrated in the light blue box. Sequence alignments were made using the T-Coffee multiple-alignment tool [50] and displayed with Jalview Version 2 [51].

4. Materials and Methods

4.1. Design of synthesized peptides

Two peptides (C3 and N1) have been described [23]. Briefly, the peptide C3 contained the C-terminal sequence of PCV2b capsid protein between residues 195 and 233, and the peptide N1 contained the sequence of PCV2b ORF3 protein between residues 35 and 66. C3 and N1 were appended with an N-terminal cysteine during synthesis, which was required for conjugation with keyhole limpet hemocyanin (Thermo scientific, Rockford, IL, USA). Other truncated peptides of N1 were used in this study which was synthesized by Yao-Hong Biotechnology Inc. (New Taipei, Taiwan) and listed in Table 1. All peptide purity was assessed by high-performance liquid chromatography (LC-10ATVP serial dual plunger pump, Shimadzu, USA) and were tested for the correct mass by Waters Micromass ZQ™ 2000 LC Mass Spectrometer (Waters, USA).

Preprints (www.preprints.org) | NOT PEER-REVIEWED | Posted: 12 November 2019 doi:10.20944/preprints201911.0131.v1

Table 1. Peptide sequences of the truncated PCV2 ORF3 protein and negative control peptide (PCV2b CP)

Name	PCV Type	Position	Peptide sequence
N1*	2b	ORF3(35-66)	CHNDVYISLPITLLHFPAHFQKFSQPAEISDKR
P31	2b	ORF3(35-44)	HNDVYISLPI
P32	2b	ORF3(45-54)	TLLHFPAHFQ
P33	2b	ORF3(55-66)	KFSQPAEISDKR
P40	2b	ORF3(40-49)	ISLPITLLHF
P41	2b	ORF3(50-59)	PAHFQKFSQP
P42	2b	ORF3(60-68)	AEISDKR**RV**
P48	2a	ORF3(35-44)	HNDVYI**G**LPI
P49	2	ORF3(35-44)	HNDVYI**R**LPI
P56	1	ORF3(35-44)	HNDVY**SC**LPI
P61	2b	ORF3(35-47)	HNDVYISLPITLL
P69	2b	ORF3(45-66)	TLLHFPAHFQKFSQPAEISDKR
P75	2b	ORF3(40-59)	ISLPITLLHFPAHFQKFSQP
P126	2b	ORF3(35-66)	HNDVYISLPITLLHFPAHFQKFSQPAEISDKR
C3*	2b	CP(195-233)	CH**VGLGTAFENSIYDQEYNIRVTMYVQFREFNL KDPPLNP**

Non-conserved amino acids are bold and underline.
* C3 and N1 were appended with an N-terminal cysteine during synthesis, which was required for conjugation with maleimide-activated carriers.

4.2. Preparation of rabbit antisera against PCV2

Antisera against PCV2 were generated by immunizing New Zealand white rabbits (from Livestock Research Institute, Council of Agriculture, Taiwan). Rabbits have maintained in isolation rooms and the room temperature was at 20–26 ℃. Rabbits were fed with a commercially pelleted diet (Fwusow In., Taiwan), and pure water was available ad libitum. This study follows the standards of the Guide of the Care and Use of Laboratory Animals and the study protocol was approved by the Committee of Animal Experimentation of Animal Health Research Institute. IACUC approval number A00027 and A02023 were given in this study. Then rabbits were immunized with peptide immunogen (peptide N1 conjugated with KLH) or commercial vaccine five times at two-week intervals. For peptide immunization, an initial dose of 150 μg of the conjugated peptide was mixed with complete Freund's adjuvant (Sigma-Aldrich, USA) at first inoculation. Each rabbit was re-immunized with the same amount of immunogenic mixture with incomplete Freund's adjuvant (Sigma-Aldrich, USA). For virus-like particles (VLP) of PCV2 immunization, the rabbit was injected intramuscularly in legs with 0.5 mL of the PCV2 vaccine (CircoFLEX®, Boehringer Ingelheim). Blood was harvested two weeks after the last inoculation. The antibody titers were measured by indirect enzyme-linked immunosorbent assay (iELISA).

4.3. Generation of mAbs against the ORF3 peptide (N1)

Hybridomas were generated following established methods as previously described [30]. Briefly, four five-week-old, female, BALB/cByJNarl mice were purchased from a specific pathogen-free (SPF) colony (the National Applied Research Laboratories, Taiwan). SPF status was verified by bacteriology, parasitology, histopathology, serology, and genetic testing through the supplier and no specific pathogens (Ectromelia virus, Hantaan virus, Lymphocytic choriomeningitis virus, Minute virus of mice, Mouse adenovirus, Mouse hepatitis virus, Mouse norovirus, Mouse parvovirus, Pneumonia virus of mice, Reovirus Type 3, Sendai virus, Theiler's murine encephalomyelitis virus, *Bordetella bronchiseptica*,

 doi:10.20944/preprints201911.0131.v1

Clostridium piliforme, *Corynebacterium kutscheri*, *Helicobacter spp.*, *Mycoplasma pulmonis*, *Pneumocystis spp.*, *Salmonella spp.*, Ecto-parasite, *Aspiculuris* tetraptera, *Giardia spp.*, *Hymenolepis diminuta*, *Rodentolepis nana*, *Spironucleus spp.*, and *Syphacia spp.*) were detected. Mice were maintained in isolation rooms in filtertop cages and the room temperature was at 20–26 ℃. Mice were fed with a commercially pelleted diet (LabDiet, 5002, USA), and pure water was available ad libitum. Mice were immunized subcutaneously with 65 μg of immunogen (peptide N1 conjugated with KLH) emulsified in complete Freund's adjuvant and boosted fortnightly with immunogen emulsified in incomplete Freund's adjuvant. Three days after the final booster, spleen cells from the mouse and mouse myeloma SP2/0 cells were fused and selected in hypoxanthin–aminopterin–thymidine (HAT) medium. Hybridomas were screened for secretion of anti-N1-specific mAbs by iELISA using N1 as a coating antigen. The hybridomas that secreted anti-N1 mAbs were then cloned by limited dilution of the cells. Then ascites containing mAbs were collected as previously described [30].

All experiments in this study were performed in accordance with relevant national laws and animal welfare requirements. All animal experiments were approved by the Committee of Animal Experimentation of Livestock Research Institute and the Committee of Animal Experimentation of Animal Health Research Institute. IACUC approval number LRIIACUC100-33, A00027, and A02023 were given in this study.

4.4. Isotyping of mAbs

The heavy chain and light chain of the two mAbs secreted by each hybridoma were determined using an SBA Clonotyping System/HRP (Southern Biotechnology, Birmingham, AL, USA). A sandwich immunoassay was performed according to the manufacturer's instructions. Briefly, the Nunc MaxiSorp flat-bottom 96 well plates (Thermo Fisher Scientific, Inc., USA) was coated with the capture antibody (goat anti-mouse Ig, 5 μg/mL) in 0.05 M bicarbonate buffer (Sigma-Aldrich, USA) at 4℃ overnight. After three washes with PBS containing 0.05% Tween 20 (PBST), the plate was blocked with PBST containing 5% casein hydrolysate at 37℃ for 60 min. After washing, 100 μL of each hybridoma culture supernatant was added sequentially, and the plate was again incubated at 37 ℃ for 2 h. After washing, 100 μL of HRP labeled goat anti-mouse IgG1, -IgG2a, -IgG2b, -IgG3, -IgA, -IgM, -κ light chain, and -λ light chain were added to appropriate wells of the plate. PBST served as background. The plate was then incubated at 37 ℃ for 1 h and thereafter washed with PBST. Finally, 100 μL of ABTS solution (Sigma-Aldrich, USA) was added to each well of the plate. After 30 min, the optical density of each well was measured at 405 nm using a SpectraMax M5 microplate reader (Molecular Devices, USA).

4.5. Hybridomas screening and epitope mapping

Hybridomas screening and epitope mapping were determined using an iELISA with peptides (as shown in Table 1) as coating antigens. Peptides contained the N-terminal sequence of PCV2b ORF3 protein between residues 35 and 66, associated 10-mer peptides, and truncated derivatives. Ninety-six-well Maxisorp plates were coated with each peptide (5 μg/mL) in bicarbonate buffer and incubated at 4 ℃ overnight. After three washes in PBST, the plates were blocked with PBST containing 5% casein hydrolysate at 37 ℃ for 30 min. After washing, the hybridoma culture supernatant was added and plates were again incubated at 37 ℃ for 2 h. After rinsing three times with PBST, HRP-conjugated goat anti-mouse IgA/IgG/IgM, H/L chain (Novus, USA) was used at 1:2500 dilution for hybridoma screening. According to the isotype of each mAb, the appropriate secondary antibody diluted solution was added for epitope mapping. Peroxidase-conjugated goat anti-mouse IgG (subclasses 1+2a+2b+3, Fcγ, Jackson ImmunoResearch, USA) was used at 1:2500 dilution; and HRP-conjugated goat anti-mouse lambda light chain (Novus, USA) was used at 1:5000 dilution. After 1 h, the plates were washed three times. The colorimetric reaction was developed using ABTS solution. The plates were read after 30 min at 405 nm.

4.6. PCV2-infected PBMCs were fixed on slides

 doi:10.20944/preprints201911.0131.v1

Homemade immunofluorescence assay (IFA) slides were performed as previously described [30] employing fetal bovine serum to fix PCV2-infected peripheral blood mononuclear cells (PBMCs) on glass slides. PBMCs were collected from PCV2-infected conventional piglets. Pig sera were detected seropositive for PCV2 by anti-C3 specific immunoassay [23] or IFA with Porcine Circovirus Type 2 (PCV2) FA Substrate Slide (VMRD, USA), and confirmed as positive for PCV2 DNA by PCR. Briefly, PBMCs were isolated from EDTA treated whole blood samples by Ficoll-Paque Plus (GE Healthcare Bio-Sciences, Uppsala, Sweden) and according to the manufacturer's instructions. The PBMCs were resuspended in fetal bovine serum. An aliquot (25 μL) of PBMCs mixture was loaded onto a glass slide for cell smear. Slides were fixed with PBS containing 2% paraformaldehyde at 4 ℃ for 10 min and then washed three times with PBS. Following slides were soaked in PBS containing 0.1% Triton X-100 at 4 ℃ for 3 min, slides were washed with PBS and prepared for IFA.

4.7. IFA of PCV2-infected PBMCs

Three anti-C3 monoclonal antibodies (1H3, 3B2, and 6B8) [30], one monoclonal anti-PCV2 antibody (36A9, Ingenasa, Madrid, Spain), polyclonal anti-p53 protein (wt-p53) antibody (Bioss, USA), and home-made monoclonal or polyclonal antibody as the aforementioned method were used in this study. The PCV2-infected PBMCs slides were incubated with a 1:100 dilution of a rabbit antibody and a 1:100 dilution of mAb. After incubation at 37 ℃ for 1 h, slides were gently rinsed briefly in PBS and then soaked for 15 minutes in PBS at 4 ℃. The slides were then incubated at 37 ℃ with TRITC-conjugated goat anti-mouse IgG (subclasses 1+2a+2b+3, Fcγ) at 1: 100 dilution, and FITC-conjugated goat anti-rabbit IgG (H+L) (all from Jackson ImmunoResearch, USA, and each antibody minimal cross-reaction to other animal's serum protein) at 1: 100 dilution. After 30 minutes of incubation, the slide was washed with PBS and then incubated with 4,6-Diamidino-2-phenylindole, dihydrochloride (DAPI, AAT Bioquest, Sunnyvale, CA, USA) at 1: 2300 dilution in PBS at room temperature for 15 min. Slides were mounted under 50% glycerol and observed with an Olympus BX51 fluorescence microscope and SPOT FlEX camera (Diagnostic Instrument, Model 15.2 64MP, USA).

4.8. Immunobinding interference detection method (IIDM)

An immunobinding interference detection method (IIDM) was developed by Ling-Chu Hung and introduced for detecting chemical interfere with the binding of specific mAb to its epitope in this study. Two anti-C3 mAbs (3B2 and 8A3) [30] and two anti-N1 mAbs (6D10 and 7D3) were used in this study. Thimerosal (2-[(Ethylmercury) Thio] Benzoic Acid Sodium Salt) was purchased from Panreac (Spain). Sodium azide was purchased from Sigma-Aldrich (USA). Ninety-six-well Maxisorp plates were coated with 5 μg/mL (100 μL per well) of the peptide (N1 or C3) in bicarbonate buffer and incubated at 4 ℃ overnight. After three washes with PBST, the plates were blocked with PBST containing 5% casein hydrolysate at 37 ℃ for 30 min. After washing, 99 μL of hybridoma culture supernatant or 1:1000 dilution of ascites (or mouse antiserum) was added to the well and 1 μL of serial dilution (100 μg/μL to 0.1 μg/μL) of thimerosal solution (or sodium azide solution) was added to the appropriate well. The plates were incubated at 37 ℃ for 2 h. After washing, 100 μL of appropriate secondary antibody diluted solution (peroxidase-conjugated goat anti-mouse IgG, or HRP-conjugated goat anti-mouse lambda light chain, and each secondary antibody was according to isotype of mAbs) were added, respectively. The plates were incubated at 37 ℃ for 1 h. After washing, assays were developed using ABST buffer. Following a 30 min incubation, the absorbance was measured at 405 nm.

4.9. Identification of thimerosal interacting- peptide or amino acid

The assay of thimerosal interacting-element truncated peptides of N1 or amino acids were performed using the blocking-IIDM (bIIDM) as the aforementioned method, with minor modification. This assay is based upon specific blocking of thimerosal by preincubating with truncated peptides of N1 or amino acids. Arginine (R), asparagine (N), aspartic acid (D), cysteine (C), glutamine (Q), glutamic

 doi:10.20944/preprints201911.0131.v1

acid (E), glycine (G), histidine (H), lysine (K), phenylalanine(F), proline (P), serine (S), and tyrosine (Y) were purchased from Sigma-Aldrich (USA). Briefly, ELISA plates were coated with peptide N1 or P126 in bicarbonate buffer at 5 μg/mL and incubated at 4 ℃ overnight. After washing and blocking, the equal volume (50 μL/well) of the thimerosal-peptide mixture (peptide or the serial dilution of amino acid was preincubated with the thimerosal solution for 1h at 37 ℃ prior to application to the plate) and serial dilution of mAb 7D3 (50 μL/well) were added to the appropriate wells. All wells should contain 100 μL total mixture (final concentration of thimerosal should be 1 mg/mL) and the plates were incubated at 37 ℃ for 2 h. After washing in PBST, secondary peroxidase-conjugated goat anti-mouse IgG (subclasses 1+2a+2b+3, Fcγ) at 1:2500 dilution in PBST containing 0.5% BSA (PBST-B) was applied for 1h. Plates were washed again in PBST and then added ABST buffer to each well. After 30 min, the optical density (OD) was read at 405 nm.

4.10. Assays of cysteine-containing peptide interacting with thimerosal

First, IgGs were purified from the ascites using the NAb Protein G Spin Column (Thermo Scientific, USA), and collected solutions were exchanged the buffer and IgG concentrated using the Amicon Ultra 50K (Millipore, USA). The IgG concentration was determined using the Nano Photometer® (Implen, Germany). Stock solutions of 2.463 mg/mL (mAb 7D3) and 1.206 mg/ml (mAb 1H3) in PBS (pH 7.2) were used in the following studies.

Peptide and thimerosal interacting (PTI) assay was performed using thimerosal-treated peptides for coating antigen, then the following steps were similar to ELISA. Briefly, one volume of the peptide solutions (1 mg/mL) were incubated with 20 volume of thimerosal solution (100 mg/mL) or PBS (control) at 37 ℃ for 1h, followed by diluting in bicarbonate buffer to a coating concentration of 5 μg/mL peptide and 10 mg/mL thimerosal. ELISA plates were coated with 100 μL/well of the aforementioned mixture and incubated at 4 ℃ overnight. After washing and blocking, the serial dilution of mAb 7D3 was added to the appropriate well and incubated at 37 ℃ for 2 h. After washing in PBST, secondary peroxidase-conjugated goat anti-mouse IgG at 1:2500 for 1h. Plates were washed again in PBST and then added ABST buffer to each well. After 30 min, the OD was read at 405 nm.

4.10. Quantification of mAb 7D3 and thimerosal interaction

Anti-C3 mAb (1H3) [30] and anti-N1 mAbs (7D3) were purified in this assay, the method was as described above. Ninety-six-well Maxisorp plates were coated with 5 μg/mL (100 μL per well) of the peptide (P126 or P59) in bicarbonate buffer and incubated at 4 ℃ overnight. After washing and blocking, 50 μL of serial dilution of mAb (7D3 or 1H3) was added to the well and 50 μL of serial dilution of thimerosal solution was added to the appropriate well. The plates were incubated at 37 ℃ for 2 h. After washing in PBST, secondary peroxidase-conjugated goat anti-mouse IgG at 1:2500 for 1h. Plates were washed again in PBST and then added ABST buffer to each well. After 30 min, the OD was read at 405 nm.

4.10. Statistical analysis

Average OD values were compared using one-way analysis of variance (ANOVA) and Tukey's Studentized Range (HSD, honestly significance difference) multiple comparisons test using the SAS Enterprise Guide 7.1® software (SAS Institute Inc., Cary, NC, USA). A p-value < 0.05 was considered significant.

5. Conclusions

The mAbs against ORF3 protein (residues 35–65) of PCV2 were generated in this study. In the relevant in vivo situation, the mAb 7D3 recognized ORF3 protein existed in PCV2-infected apoptotic porcine PBMCs. The data displayed that the binding affinity of mAb 7D3 was sensitive to thimerosal treatment. It is noted that the only cysteine diminished the strength of thimerosal interacting with

 doi:10.20944/preprints201911.0131.v1

mAb 7D3. Moreover, thimerosal specifically interacted with the antigen-binding sites of mAb 7D3. The lower limit of detection of the thimerosal interacting with mAb 7D3 was 10 μg/mL. This study suggested that thimerosal blockade the occlusion of the antigen-binding sites of mAb 7D3 to bind peptide P126 (ORF3 protein residues 35–65) via thimerosal interacting with cysteine residues which are located within the antigen-binding sites of mAb 7D3. Taken together, the mAb 7D3 has been characterized and it will be a valuables tool in future studies of ORF3 protein function and the wider mechanism of cell apoptosis caused by PCV2 infection. Similarly, researchers could apply these techniques to detect the active form of thimerosal content in thimerosal-containing solutions or vaccines in times to come.

Author Contributions: Conceptualization, methodology, validation, formal analysis, investigation, resources, data curation, writing—original draft preparation, writing—review and editing, visualization, supervision, project administration, funding acquisition, L.-C.H.

Funding: This work was supported by the grant from Livestock Research Institute (100AS-2.1.1-LI-L1) and by grants from Animal Health Research Institute (106AS-2.1.3-HI-H1 and 107AS-2.1.3-HI-H1).

Acknowledgments: Dr. Ming-Yang Tsia, Dr. Jenn-Rong Yang, Dr. Tzong-Faa Shiao (Livestock Research Institute), and Dr. Chu-Hsiang Pan (Animal Health Research Institute) are thanked for kindly providing experimental equipment and facilities.

Conflicts of Interest: The author declares no conflict of interest.

Abbreviations

ANOVA	Analysis of variance
bIIDM	Blocking immunobinding interference detection method
CP	Capsid protein
Cterminus	Carboxyl-terminus
DMEM	Dulbecco's modified Eagle medium
IIDM	Immunobinding interference detection method
iELISA	Indirect enzyme-linked immunosorbent assay
IFA	Immunofluorescence assay
Ig	Immunoglobulin
KLH	Keyhole limpet hemocyanin
mAb	Monoclonal antibody
OD	Optical density
ORF	Open reading frames
PBMCs	Peripheral blood mononuclear cells
PBST	PBS containing 0.05% Tween 20
PCV	Porcine circovirus
PCV1	Porcine circovirus type 1
PCV2	Porcine circovirus type 2
PDNS	Porcine dermatitis and nephropathy syndrome
PEG	Polyethylene glycol
PMWS	Post-weaning multisystemic wasting syndrome
pPirh2	Porcine p53-induced RING-H2
PTI	Peptide and thimerosal interacting
SCF	Suspending cells were fixed
SPF	Specific pathogen-free
Thi	Thimerosal
TRITC	Tetramethyl rhodamine isothiocyanate;
VLP	Virus-like particle

References

1. Tischer, I.; Gelderblom, H.; Vettermann, W.; Koch, M.A. A very small porcine virus with circular single-stranded DNA. *Nature* **1982**, *295*, 64.
2. Meehan, B.M.; McNeilly, F.; Todd, D.; Kennedy, S.; Jewhurst, V.A.; Ellis, J.A.; Hassard, L.E.; Clark, E.G.; Haines, D.M.; Allan, G.M. Characterization of novel circovirus DNAs associated with wasting syndromes in pigs. *J. Gen. Virol.* **1998**, *79 (Pt 9)*, 2171–2179.
3. Tischer, I.; Mields, W.; Wolff, D.; Vagt, M.; Griem, W. Studies on epidemiology and pathogenicity of porcine circovirus. *Arch. Virol.* **1986**, *91*, 271–276.
4. Allan, G.M.; Kennedy, S.; McNeilly, F.; Foster, J.C.; Ellis, J.A.; Krakowka, S.J.; Meehan, B.M.; Adair, B.M. Experimental reproduction of severe wasting disease by co-infection of pigs with porcine circovirus and porcine parvovirus. *J. Comp. Pathol.* **1999**, *121*, 1–11.
5. Kennedy, S.; Moffett, D.; McNeilly, F.; Meehan, B.; Ellis, J.; Krakowka, S.; Allan, G.M. Reproduction of lesions of postweaning multisystemic wasting syndrome by infection of conventional pigs with porcine circovirus type 2 alone or in combination with porcine parvovirus. *J. Comp. Pathol.* **2000**, *122*, 9–24.
6. Segalés, J.; Domingo, M. Postweaning mulstisystemic wasting syndrome (PMWS) in pigs. A review. *Veterinary Quarterly* **2002**, *24*, 109–124.
7. Kim, J.; Ha, Y.; Jung, K.; Choi, C.; Chae, C. Enteritis associated with porcine circovirus 2 in pigs. *Can J Vet Res* **2004**, *68*, 218–221.
8. Opriessnig, T.; Meng, X.-J.; Halbur, P.G. Porcine circovirus type 2 associated disease: update on current terminology, clinical manifestations, pathogenesis, diagnosis, and intervention strategies. *J. Vet. Diagn. Invest.* **2007**, *19*, 591–615.
9. Segalés, J. Porcine circovirus type 2 (PCV2) infections: Clinical signs, pathology and laboratory diagnosis. *Virus Research* **2012**, *164*, 10–19.
10. Hamel, A.L.; Lin, L.L.; Nayar, G.P.S. Nucleotide Sequence of Porcine Circovirus Associated with Postweaning Multisystemic Wasting Syndrome in Pigs. *Journal of Virology* **1998**, *72*, 5262–5267.
11. Cheung, A.K. The essential and nonessential transcription units for viral protein synthesis and DNA replication of porcine circovirus type 2. *Virology* **2003**, *313*, 452–459.
12. Nawagitgul, P.; Morozov, I.; Bolin, S.R.; Harms, P.A.; Sorden, S.D.; Paul, P.S. Open reading frame 2 of porcine circovirus type 2 encodes a major capsid protein. *Journal of General Virology* **2000**, *81*, 2281–2287.
13. Liu, J.; Chen, I.; Kwang, J. Characterization of a Previously Unidentified Viral Protein in Porcine Circovirus Type 2-Infected Cells and Its Role in Virus-Induced Apoptosis. *Journal of Virology* **2005**, *79*, 8262–8274.
14. Liu, J.; Chen, I.; Du, Q.; Chua, H.; Kwang, J. The ORF3 protein of porcine circovirus type 2 is involved in viral pathogenesis in vivo. *J. Virol.* **2006**, *80*, 5065–5073.
15. Karuppannan, A.K.; Jong, M.H.; Lee, S.-H.; Zhu, Y.; Selvaraj, M.; Lau, J.; Jia, Q.; Kwang, J. Attenuation of porcine circovirus 2 in SPF piglets by abrogation of ORF3 function. *Virology* **2009**, *383*, 338–347.

16. Liu, J.; Zhu, Y.; Chen, I.; Lau, J.; He, F.; Lau, A.; Wang, Z.; Karuppannan, A.K.; Kwang, J. The ORF3 protein of porcine circovirus type 2 interacts with porcine ubiquitin E3 ligase Pirh2 and facilitates p53 expression in viral infection. *J. Virol.* **2007**, *81*, 9560–9567.
17. Karuppannan, A.K.; Liu, S.; Jia, Q.; Selvaraj, M.; Kwang, J. Porcine circovirus type 2 ORF3 protein competes with p53 in binding to Pirh2 and mediates the deregulation of p53 homeostasis. *Virology* **2010**, *398*, 1–11.
18. Choi, C.-Y.; Rho, S.B.; Kim, H.-S.; Han, J.; Bae, J.; Lee, S.J.; Jung, W.-W.; Chun, T. The ORF3 protein of porcine circovirus type 2 promotes secretion of IL-6 and IL-8 in porcine epithelial cells by facilitating proteasomal degradation of regulator of G protein signalling 16 through physical interaction. *J. Gen. Virol.* **2015**, *96*, 1098–1108.
19. Karuppannan, A.K.; Kwang, J. ORF3 of porcine circovirus 2 enhances the in vitro and in vivo spread of the of the virus. *Virology* **2011**, *410*, 248–256.
20. Stevenson, L.S.; Gilpin, D.F.; Douglas, A.; McNeilly, F.; McNair, I.; Adair, B.M.; Allan, G.M. T lymphocyte epitope mapping of porcine circovirus type 2. *Viral Immunol.* **2007**, *20*, 389–398.
21. Gu, J.; Wang, L.; Jin, Y.; Lin, C.; Wang, H.; Zhou, N.; Xing, G.; Liao, M.; Zhou, J. Characterization of specific antigenic epitopes and the nuclear export signal of the Porcine circovirus 2 ORF3 protein. *Veterinary Microbiology* **2016**, *184*, 40–50.
22. He, J.-L.; Dai, D.; Zhou, N.; Zhou, J.-Y. Analysis of Putative ORF3 Gene Within Porcine Circovirus Type 2. *Hybridoma* **2012**, *31*, 180–187.
23. Hung, L.-C.; Yang, C.-Y.; Cheng, I.-C. Peptides mimicking viral proteins of porcine circovirus type 2 were profiled by the spectrum of mouse anti-PCV2 antibodies. *BMC Immunol* **2017**, *18*, 25.
24. Abrams, J.D.; Davies, T.G.; Klein, M. MERCURIAL PRESERVATIVES IN EYE-DROPS*. *Br J Ophthalmol* **1965**, *49*, 146–147.
25. Mucciolo, P.; Lacaz, C.S.; Ribeiro, P.A. [Penicilliosis in cheese; preliminary observations on the effect of ethylmercury thiosalicylate sodium (merthiolate) for the prophylaxis of changes produced by Penicillium sp]. *Rev Fac Med Vet Univ Sao Paulo* **1948**, *3*, 283–300.
26. Powell, H.M. Antibacterial action of merthiolate against hemolytic streptococci. *J Am Med Assoc* **1948**, *137*, 862–866.
27. Simmons, R.T.; Woods, E.F. Anti-Rh human sera preserved with merthiolate. *Aust J Sci* **1946**, *8*, 108–111.
28. Xu, Y.; Pang, G.; Zhao, D.; Gao, C.; Zhou, L.; Sun, S.; Wang, B. In vitro activity of thimerosal against ocular pathogenic fungi. *Antimicrob. Agents Chemother.* **2010**, *54*, 536–539.
29. Liu, G.; Amin, S.; Okuhama, N.N.; Liao, G.; Mingle, L.A. A quantitative evaluation of peroxidase inhibitors for tyramide signal amplification mediated cytochemistry and histochemistry. *Histochem. Cell Biol.* **2006**, *126*, 283–291.
30. Hung, L.-C.; Cheng, I.-C. Versatile carboxyl-terminus of capsid protein of porcine circovirus type 2 were recognized by monoclonal antibodies with pluripotency of binding. *Mol. Immunol.* **2017**, *85*, 100–110.

31. Karuppannan, A.K.; Liu, S.; Jia, Q.; Selvaraj, M.; Kwang, J. Porcine circovirus type 2 ORF3 protein competes with p53 in binding to Pirh2 and mediates the deregulation of p53 homeostasis. *Virology* **2010**, *398*, 1–11.
32. Xu, D.; Du, Q.; Han, C.; Wang, Z.; Zhang, X.; Wang, T.; Zhao, X.; Huang, Y.; Tong, D. p53 signaling modulation of cell cycle arrest and viral replication in porcine circovirus type 2 infection cells. *Vet Res* **2016**, *47*, 120.
33. Kiupel, M.; Stevenson, G.W.; Galbreath, E.J.; North, A.; HogenEsch, H.; Mittal, S.K. Porcine circovirus type 2 (PCV2) causes apoptosis in experimentally inoculated BALB/c mice. *BMC Vet. Res.* **2005**, *1*, 7.
34. Liu, G.; Wang, Y.; Jiang, S.; Sui, M.; Wang, C.; Kang, L.; Sun, Y.; Jiang, Y. Suppression of lymphocyte apoptosis in spleen by CXCL13 after porcine circovirus type 2 infection and regulatory mechanism of CXCL13 expression in pigs. *Veterinary Research* **2019**, *50*, 17.
35. Resendes, A.R.; Majó, N.; Segalés, J.; Mateu, E.; Calsamiglia, M.; Domingo, M. Apoptosis in lymphoid organs of pigs naturally infected by porcine circovirus type 2. *J. Gen. Virol.* **2004**, *85*, 2837–2844.
36. Segalés, J.; Domingo, M.; Chianini, F.; Majó, N.; Dominguez, J.; Darwich, L.; Mateu, E. Immunosuppression in postweaning multisystemic wasting syndrome affected pigs. *Vet. Microbiol.* **2004**, *98*, 151–158.
37. Lin, W.-L.; Chien, M.-S.; Wu, P.-C.; Lai, C.-L.; Huang, C. The Porcine Circovirus Type 2 Nonstructural Protein ORF3 Induces Apoptosis in Porcine Peripheral Blood Mononuclear Cells. *Open Virol J* **2011**, *5*, 148–153.
38. Liu, J.; Chen, I.; Kwang, J. Characterization of a Previously Unidentified Viral Protein in Porcine Circovirus Type 2-Infected Cells and Its Role in Virus-Induced Apoptosis. *Journal of Virology* **2005**, *79*, 8262–8274.
39. Hough, K.P.; Rogers, A.M.; Zelic, M.; Paris, M.; Heilman, D.W. Transformed cell-specific induction of apoptosis by porcine circovirus type 1 viral protein 3. *J. Gen. Virol.* **2015**, *96*, 351–359.
40. Tan, M.; Parkin, J.E. Route of decomposition of thiomersal (thimerosal). *International Journal of Pharmaceutics* **2000**, *208*, 23–34.
41. Roesijadi, G. Mercury-binding proteins from the marine mussel, Mytilus edulis. *Environ. Health Perspect.* **1986**, *65*, 45–48.
42. Trümpler, S.; Lohmann, W.; Meermann, B.; Buscher, W.; Sperling, M.; Karst, U. Interaction of thimerosal with proteins—ethylmercuryadduct formation of human serum albumin and β-lactoglobulin A. *Metallomics* **2009**, *1*, 87–91.
43. Santos, J.C.N.; da Silva, I.M.; Braga, T.C.; de Fátima, Â .; Figueiredo, I.M.; Santos, J.C.C. Thimerosal changes protein conformation and increase the rate of fibrillation in physiological conditions: Spectroscopic studies using bovine serum albumin (BSA). *Int. J. Biol. Macromol.* **2018**, *113*, 1032–1040.
44. Chen, S.; Huang, X.; Li, Y.; Wang, X.; Pan, H.; Lin, Z.; Zheng, Q.; Li, S.; Zhang, J.; Xia, N.; et al. Altered antigenicity and immunogenicity of human papillomavirus virus-like particles in the presence of thimerosal. *Eur J Pharm Biopharm* **2019**, *141*, 221–231.

 doi:10.20944/preprints201911.0131.v1

45. Leng, R.P.; Lin, Y.; Ma, W.; Wu, H.; Lemmers, B.; Chung, S.; Parant, J.M.; Lozano, G.; Hakem, R.; Benchimol, S. Pirh2, a p53-Induced Ubiquitin-Protein Ligase, Promotes p53 Degradation. *Cell* **2003**, *112*, 779–791.
46. Sheng, Y.; Laister, R.C.; Lemak, A.; Wu, B.; Tai, E.; Duan, S.; Lukin, J.; Sunnerhagen, M.; Srisailam, S.; Karra, M.; et al. Molecular basis of Pirh2-mediated p53 ubiquitylation. *Nat. Struct. Mol. Biol.* **2008**, *15*, 1334–1342.
47. Attallah, C.; Aguilar, M.F.; Garay, A.S.; Herrera, F.E.; Etcheverrigaray, M.; Oggero, M.; Rodrigues, D.E. An unusual cysteine VL87 affects the antibody fragment conformations without interfering with the disulfide bond formation. *Mol. Immunol.* **2017**, *90*, 143–149.
48. Gao, X.; Yeo, K.P.; Aw, S.S.; Kuss, C.; Iyer, J.K.; Genesan, S.; Rajamanonmani, R.; Lescar, J.; Bozdech, Z.; Preiser, P.R. Antibodies targeting the PfRH1 binding domain inhibit invasion of Plasmodium falciparum merozoites. *PLoS Pathog.* **2008**, *4*, e1000104.
49. Londergan, C.H.; Baskin, R.; Bischak, C.G.; Hoffman, K.W.; Snead, D.M.; Reynoso, C. Dynamic asymmetry and the role of the conserved active-site thiol in rabbit muscle creatine kinase. *Biochemistry* **2015**, *54*, 83–95.
50. Di Tommaso, P.; Moretti, S.; Xenarios, I.; Orobitg, M.; Montanyola, A.; Chang, J.-M.; Taly, J.-F.; Notredame, C. T-Coffee: a web server for the multiple sequence alignment of protein and RNA sequences using structural information and homology extension. *Nucleic Acids Res.* **2011**, *39*, W13-17.
51. Waterhouse, A.M.; Procter, J.B.; Martin, D.M.A.; Clamp, M.; Barton, G.J. Jalview Version 2—a multiple sequence alignment editor and analysis workbench. *Bioinformatics* **2009**, *25*, 1189–1191.